

Plate Acceleration and Sound Transmission Due to Random Acoustic and Boundary-Layer Excitation

Ferdinand W. Grosveld*

Lockheed Engineering & Sciences Company, Hampton, Virginia 23666

The VAPEPS statistical energy analysis model is used in the frequency range of 315–5000 Hz to predict the acceleration response and sound transmission of plates that are exposed to random acoustic or turbulent boundary-layer excitation. Good agreement was found with measured noise reduction data for aluminum, acrylic, and graphite-epoxy plates with length and width larger than the acoustic wavelength. The VAPEPS predicted acceleration response of a $12 \times 8 \times 0.040$ -in. plate, installed in a 1-in. thick rigid plate inside a wind tunnel, agreed well with measured data for a stationary (random acoustic) as well as for a convected (turbulent boundary layer) pressure field. It was found that lowest order plate modal frequencies increase most with free flow velocity U . The overall acceleration level as well as the transmitted sound pressure level due to turbulent boundary-layer excitation were close to a $U^{5.0}$ dependence. Excitation by a laminar boundary layer resulted in a $U^{3.6}$ dependence. Measured noise reduction data for random acoustic excitation of the plate in the wind tunnel fell between the VAPEPS predicted curves for resonant and nonresonant sound transmission showing the limitations of statistical energy analysis to accurately predict sound transmission at low modal densities. The noise reduction of the plate, when backed by a shallow cavity and excited by a turbulent boundary layer, was predicted using a simplified theory based on the assumption of adiabatic compression of the fluid in the cavity. VAPEPS predicted plate acceleration response was used as input in the noise reduction prediction, and reasonable agreement was found with the measured noise reduction in the frequency range of 315–1000 Hz.

Introduction

THE convected field of unsteady pressure fluctuations in a turbulent boundary layer on the exterior of aircraft and launch vehicles induces structural vibrations that radiate sound into the interior acoustic space. Another contributor to the interior noise in these vehicles is the radiation of acoustic waves from the engine exhaust, which excites the exterior of the structure and then couples with the interior acoustic space. To facilitate sound transmission tests in a reverberation chamber, the engine exhaust noise is often modeled as a diffuse random acoustic source. The objective of this paper is to investigate the acceleration response and noise reduction of flat plates when excited by random acoustic or turbulent boundary-layer excitation. To achieve this objective a statistical energy analysis method is employed, and the assumptions at the basis of that approach are examined.

Prediction Methodology

Statistical Energy Analysis (SEA) is based on the net power flow between two or more coupled mechanical and/or acoustical systems excited by broadband random forces. From the kinetic and potential energy balance between participating modes in a frequency band, the mean-square value of the dynamic response can be determined. Statistical energy techniques were first employed in the early 1960s by Lyon and Maidanik,¹ Maidanik,² and Lyon,³ and the underlying theory was later extended by Lyon and Eichler,⁴ Lyon and Scharton,⁵ Ungar and Scharton,⁶ and others. Crocker and Price⁷ and Price and Crocker⁸ developed a technique to use SEA in predicting the sound transmission loss, the radiation resistance, and the vibration

amplitude of single and double panels. The SEA concept is used in the theoretical prediction scheme of the VibroAcoustic Payload Environment Prediction System (VAPEPS), which was developed by Lockheed Missiles & Space Company⁹ under the auspices of NASA. Improvement and expansion of VAPEPS is sponsored by the United States Air Force Space Division and managed by the Jet Propulsion Laboratory.¹²

Vibrating mechanical or acoustic systems are described in VAPEPS as members of a statistical population. The VAPEPS program allows modeling of a complex structure by subsystems of plates, cylinders, and cones. Many point, line, and area connections between these subsystems are possible within VAPEPS to describe their mutual coupling. The acoustic space is modeled by its volume, area, impedance, and loss factor. Both resonant and nonresonant energy paths are supported. The prediction scheme takes the structural, acoustic, and excitation parameters and provides an energy balance from which the one-third octave band mean-square value of the response can be determined.

Recently, the capability of calculating acceleration response and sound transmission due to turbulent boundary-layer excitation has been added to the VAPEPS model.¹³ The attached turbulent boundary layer is idealized as a progressive wave to represent the convecting fluctuating pressure field. This pressure field depends on the undisturbed flow velocity and the properties of the convecting eddies. The variation in the size of these eddies, their inherent different convection velocities, different duration of coherence, and different extent of the eddy decay time have been ignored to simplify the analysis. It is assumed that the fluctuating pressure field is statistically homogeneous, is stationary in time and space, and is convected in the direction of the flow with a velocity U_c . The wavenumber and frequency spectrum of the fluctuating pressure field is given by¹³

$$\phi_p(k, \omega) = \bar{P}_n^2 \phi_{13}(k) \phi_m(\omega - k_1 U_c)$$

where \bar{P}_n^2 is the overall mean-square pressure, $\phi_{13}(k)$ is the normalized wavenumber spectrum that characterizes the distribution of eddy size, k_1 and k_3 are components in the direc-

Received Sept. 6, 1990; presented as Paper 90-3964 at the AIAA 13th Aeroacoustics Conference, Tallahassee, FL, Oct. 22–24, 1990; revision received April 1, 1991; accepted for publication April 12, 1991. Copyright © 1990 by F. W. Grosveld. Published by the American Institute of Aeronautics and Astronautics, Inc., with permission.

*Section Manager, Aeroacoustics and Structural Acoustics, 144 Research Drive. Associate Fellow AIAA.

tion of the flow and transverse to the flow, and $\phi_m(\omega - k_1 U_c)$ is the moving axis spectrum that describes the temporal decay of the eddies. The power transfer from the pressure field to a plate or a cylinder is derived in VAPEPS for frequency regions above and below the hydrodynamic and acoustic coincidence frequencies.¹³

Experiments Involving Random Acoustic Excitation

Statistical energy analysis can be applied to describe the sound transmission through a plate that is excited by a reverberant acoustic field. The plate is considered to be mounted in a rigid baffle that has no flanking paths. The reverberant acoustic field will generate a homogeneous pressure field in the plane of the plate that will set the plate into vibration. Sound will then be radiated by the vibrating plate. Resonant as well as nonresonant transmission is possible, and their relative importance depends on the plate characteristics and the variation of internal and radiation resistance with frequency.⁷ When the trace wavelength of the incident acoustic waves matches the plate bending wavelength, the coupling between acoustic excitation and plate vibration is high, and the radiation efficiency equals unity. Above this critical frequency, the transmission of a reverberant field is dominated by resonance transmission associated with coincidence. Below the critical frequency, the radiation efficiency is less than one, and in addition to the resonance transmission, there is a forced vibration contribution. The transmission due to the nonresonant modes is known as "mass law" transmission. Well above the critical frequency, internal damping increases rapidly, and the transmission again approaches mass law. Only the frequency region well above the fundamental resonance frequency and below the critical frequency of the plate will be considered in this paper. Plate resonant modes in this frequency region have bending wave velocities less than the speed of sound and a low radiation efficiency. When the nodal lines on the plate in two perpendicular directions are separated by less than half the acoustic wavelength, all of the volume velocities are canceled except in the corners, and therefore, only corner modes will radiate sound. Edge modes will occur when nodal lines in only one direction are separated by less than half the acoustic wavelength. Corner modes radiate sound less efficiently than edge modes that, in turn, are less efficient than when the entire surface radiates sound (acoustically fast modes). Sound transmission experiments with broadband acoustic excitation have been conducted on plates in a transmission loss suite and in a wind tunnel without flow.

Transmission Loss Apparatus

The sound transmission experiments were conducted in the NASA Langley Transmission Loss Apparatus¹⁴ (Fig. 1). Each test plate was mounted as a partition between two reverberant rooms. A diffuse sound field was produced in the source room by two reference sound power sources and measured by a microphone mounted at the end of a rotating boom. At the same time another rotating microphone measured the sound pressure

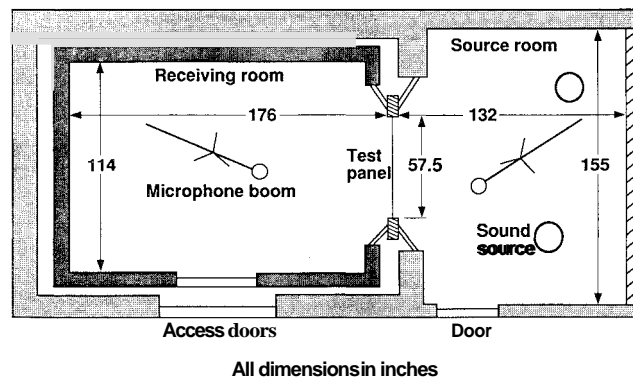


Fig. 1 Planform of the transmission loss apparatus.

levels in the receiver room. The difference in space-averaged sound pressure levels in the source and receiver rooms was defined as the noise reduction of the test plate. The noise reduction of an aluminum, an acrylic, and a graphite-epoxy plate was determined. The dimensions and material properties, used as input into the VAPEPS program, are tabulated in Table 1. Measured noise reduction is compared with VAPEPS predictions in Figs. 2–4. Previous transmission loss measurements¹⁴ indicated that all three plates behave according to mass law. The sound radiation from these plates is dominated by the forced vibration of the nonresonant modes and the contribution of the resonance modes is low by comparison. Note that the noise reduction predictions for the acrylic panel in Fig. 3 follow the measured values as they approach the critical frequency that was predicted at 5200 Hz. Agreement is within 2 dB in the lowest frequency bands and better at higher frequencies, which shows that the statistical energy approach works well for structures and acoustic spaces with high modal densities.

Wind Tunnel Without Flow

Test Configuration and Acoustic Excitation

Experiments involving acoustic broadband excitation were conducted in the 15 × 15 × 120-in. test section of a low-turbulence wind tunnel. The test section was divided into two equal volumes by a horizontally mounted 1-in. thick, rigid aluminum plate with a 12 × 8-in. cutout section to accommodate a 0.040-in. thick aluminum plate insert (Fig. 5). The objective was to describe the sound transmission through the plate when excited by the broadband sound from a loudspeaker source located in the upstream far field. To insure sound transmission through the panel in only one direction, the volume below the rigid aluminum plate was acoustically sealed by several layers of mass-loaded material (1 lb/ft²) and filled with acoustic foam. The volume above the rigid aluminum plate behind the flexible plate was also filled with acoustic foam to prevent reflections from the back of the tunnel. The response of the panel was measured by an accelerometer weighing 0.01 oz that was located on the longitudinal centerline of the flexible plate 8 in. from the forward edge (Fig. 5). The transmitted sound was measured by a microphone 2.5 in. below this accelerometer location. The flexible plate was replaced by a rigid plate with a flush-mounted microphone to measure the sound incident at the former accelerometer location. The one-third octave band excitation spectrum (315–5000 Hz) measured by the flush-mounted microphone is shown in Fig. 6. The "white noise" spectrum, which was input to the loudspeaker, was molded by acoustic modes in the test section above the flexible plate. Since the longitudinal dimension of the acoustic foam (4 ft) was longer than the acoustic wavelength at 315 Hz, it was assumed that there were no longitudinal acoustic modes and only tangential acoustic modes existed in the space above the plate. All of the odd numbered horizontal acoustic modes have a node along the centerline and (ideally) have zero fluctuating pressure at that location. Frequencies of 448, 1059, and 1972 Hz were calculated for the first three tangential modes with a node along the centerline. The 448 Hz is the acoustic cutoff frequency below which only plane wave sound may be propagated. These three frequencies coincide with dips in the one-third octave band excitation spectrum of Fig. 6. The spectrum of Fig. 6 was used as input to the VAPEPS program.

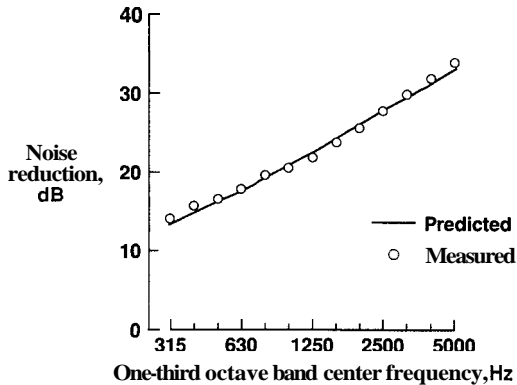
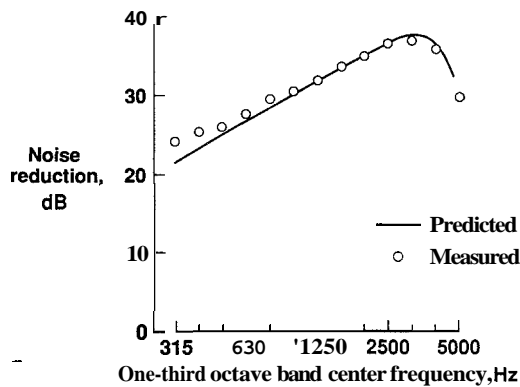
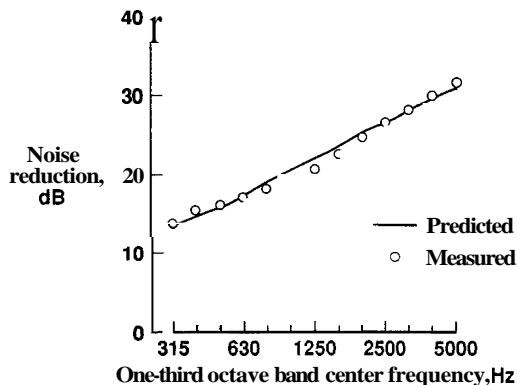
VAPEPS Prediction Constraints

The frequency region of interest was somewhat arbitrarily chosen to include the 315–5000 Hz one-third octave bands. The validity of modeling the current test configuration with VAPEPS for these frequencies needs to be addressed in view of the underlying assumptions in statistical energy analysis.¹⁹

The *fundamental plate resonance frequency* was measured at 153 Hz and calculated to occur at 154.5 Hz assuming clamped boundary conditions at its edges. The *critical frequency* of the panel, where the propagation velocity of free bending waves

Table 1 Material properties of test plates

Parameter	Plates in transmission loss facility			Plate in wind tunnel
	Aluminum	Acrylic	Graphite-epoxy	Aluminum
Density, lb s ² /in. ⁴	2.57×10^{-4}	4.14×10^{-4}	1.46×10^{-4}	2.57×10^{-4}
Thickness, in.	0.032	0.25	0.045	0.040
Length, in.	57.5	57.5	57.5	12.0
Width, in.	45.5	45.5	33.5	8.0
Young's modulus, lb/in. ²	1.03×10^7	5.80×10^5	1.02×10^7	1.03×10^7
Longitudinal wave speed, in./s	2.01×10^5	0.71×10^5	2.64×10^5	2.01×10^5

Fig. 2 Measured and VAPEPS predicted noise reduction of a $57.5 \times 45.5 \times 0.032$ -in. aluminum plate.Fig. 3 Measured and VAPEPS predicted noise reduction of a $57.5 \times 45.5 \times 0.25$ -in. acrylic plate.Fig. 4 Measured and VAPEPS predicted noise reduction of a $57.5 \times 33.5 \times 0.045$ -in. graphite-epoxy plate.

is equal to the acoustic wavespeed, is calculated from $f_c = c_0^2 / 2\pi\kappa c_\ell = 12,008$ Hz where c_0 is the speed of sound, κ is the radius of gyration, and c_ℓ is the longitudinal wavespeed in the material. The frequency region of interest lies between the fundamental resonance frequency and critical frequency and the plate will be subject to resonant as well as nonresonant sound transmission.

The *plate bending wavelength* is assumed to be small, compared with the plate width and length, and is calculated from $\lambda_p = 2\pi\sqrt{\kappa c_\ell / \omega}$ where $\omega = 2\pi f$. At 315 Hz the plate bending wavelength is 6.8 in., which is smaller than the plate width of $b = 8$ in.

The *plate modal density* was calculated by the VAPEPS model to be 0.021 based on simply supported edge conditions of the plate. Actual boundary conditions are very close to clamped. Computing individual modal frequencies for a clamped $12 \times 8 \times 0.040$ -in. aluminum plate suggests that only one mode is resonant in the 325 Hz one-third octave band. This is the minimum required for resonant sound transmission.

The *wave numbers* for the m and n modes of vibration are given by $k_m = m\pi/a = 0.26$ m 1/in. and $k_n = n\pi/b = 0.39$ n 1/in., where a and b are the length and the width of the panel. The radiated sound waves in air have a wave number $k_0 = 2\pi f/c_0 = 4.67 \times 10^{-4}f$. Below the critical frequency, VAPEPS employs an edge mode radiation model for the resonant sound transmission. Both edge and corner modes occur when either $k_m < k_0$ or $k_n < k_0$. When both wave numbers are greater than the acoustic wave number in air, volume velocity cancellation will take place in two directions, leaving only corner modes to radiate sound. When the panel is much less than a wavelength ($ka < 1$ or $kb < 1$), edge modes do not exist, and corner modes will interact with each other to radiate together as a monopole, dipole, or quadrupole depending on their phase relationships. However, at 315 Hz and higher frequencies, both ka and kb are greater than 1.

Excitation Response

In Fig. 7 the mean-square acceleration power spectral density is plotted as a function of frequency for the location indicated in Fig. 5 and the excitation spectrum shown in Fig. 6. This excitation spectrum was used as input into the VAPEPS model to calculate mean-square acceleration power spectral density in one-third octave bands. This calculated spectrum is also plotted in Fig. 6 and compares well with the measured data. The noise reduction between the excitation spectrum of Fig. 6 and the transmitted sound spectrum measured by the microphone underneath the plate is shown in Fig. 8. The VAPEPS model was used to predict noise reduction of the plate for both resonant and nonresonant transmission. The foam-treated receiving cavity was modeled as an anechoic space with an absorption coefficient of unity. The resulting calculated noise reduction values, also plotted in Fig. 8, provide upper and lower bounds for the measured data. The lower predicted noise reduction curve represents the forced response of a limp infinite plate. The plate, however, is not infinite and is much affected by the restraints at its boundaries. Due to reflections at these boundaries, the resonant sound transmission becomes impor-

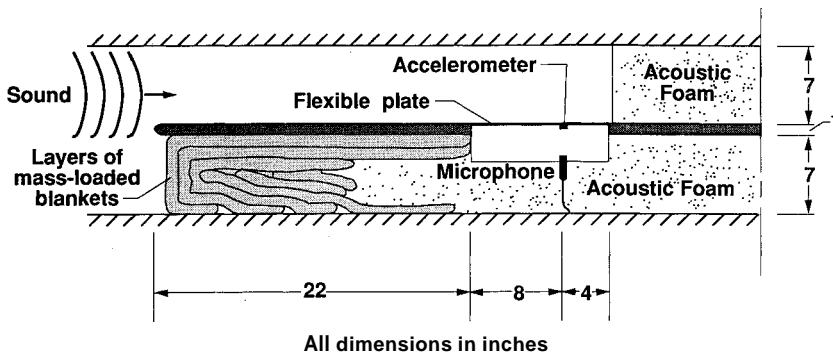


Fig. 5 Test configuration of a 12 x 8 x 0.040-in. aluminum plate subjected to broadband acoustic excitation in a wind tunnel with no flow.

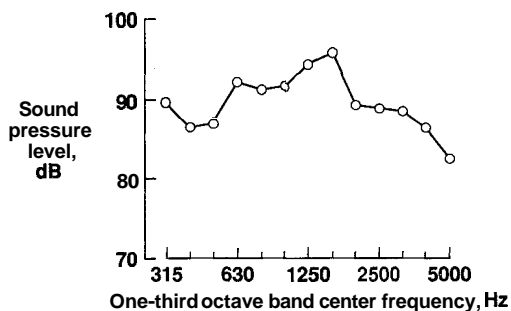


Fig. 6 Measured loudspeaker generated acoustic excitation spectrum incident on the flexible aluminum plate in the wind tunnel.

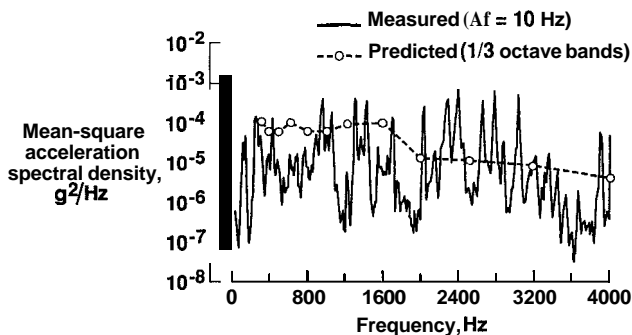


Fig. 7 Measured and VAPEPS predicted mean-square acceleration spectral density of the plate in the wind tunnel due to broadband acoustic excitation.

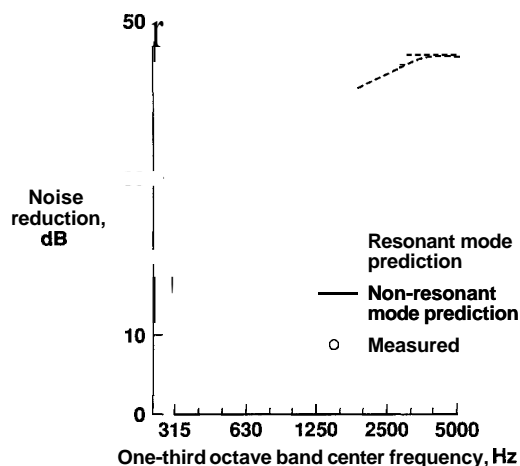


Fig. 8 Measured and VAPEPS predicted resonant and nonresonant noise reduction of the flexible plate in the wind tunnel due to broadband acoustic excitation.

tant relative to nonresonant transmission, and measured data will not coincide with either prediction.

Experiments Involving Turbulent Boundary-Layer Excitation

Test Configuration

The mass-loaded material and acoustic foam were removed from the wind tunnel to accommodate turbulent boundary-layer excitation of the plate. A 2-in. deep metal cover was positioned underneath the flexible plate and attached to the rigid plate to allow only one side of the plate to be excited by the boundary flow (Fig. 9). Several layers of mass-loaded blankets were placed over the metal cover, acoustically sealing the enclosed cavity to prevent or reduce flanking paths. A microphone was positioned inside the cover at the same location of the microphone used in the broadband acoustic excitation tests. The low turbulence wind tunnel was capable of free flow velocities up to 110 ft/s or approximately Mach = 0.098. The transition from laminar to turbulent boundary-layer flow was measured by a hot-wire anemometer at 54.5 ft/s just above the accelerometer location (Fig. 9).

Boundary-Layer Excitation

The flexible plate was temporarily replaced by a rigid plate with a flush-mounted microphone to measure the boundary-layer excitation in one-third octave bands. Figure 10 shows the excitation spectra for several tunnel speeds at which the boundary layer was turbulent. These spectra are relatively smooth without the tangential acoustic tunnel modes as were observed in the case of broadband acoustic excitation (Fig. 6). The sound pressure level seems to increase linearly with freestream velocity in each frequency band. Hydrodynamic coincidence occurs at frequencies where the flexural plate modal wave number in the direction of the flow matches the wave number of the hydrodynamic perturbances that move along the plate surface with convection velocity U_c . This coincidence condition with mode m in the direction of flow is defined by the relationship $(k_m - U_c/2\kappa c_t)^2 + k_n^2 = (U_c/2\kappa c_t)^2$ where $U_c = 0.75U$ and the undisturbed flow speed $U = 110$ ft/s.

VAPEPS Model

The hydrodynamic coincidence occurs at frequencies lower than the frequency range of the present analysis, which means that no special modes are well excited and all the plate modes share in the average response. This type of vibration is controlled by the temporal decay of the pressure eddies and is described in the VAPEPS model by the moving-axis spectrum^{9,21}

$$\phi_m(\omega - U_c k_1) = \frac{2}{\pi} \frac{0}{1 + \theta^2(\omega - U_c k_1)^2}$$

which corresponds to a moving-axis eddy decay model

$$\phi(\tau) = e^{-|\tau|/\theta}$$

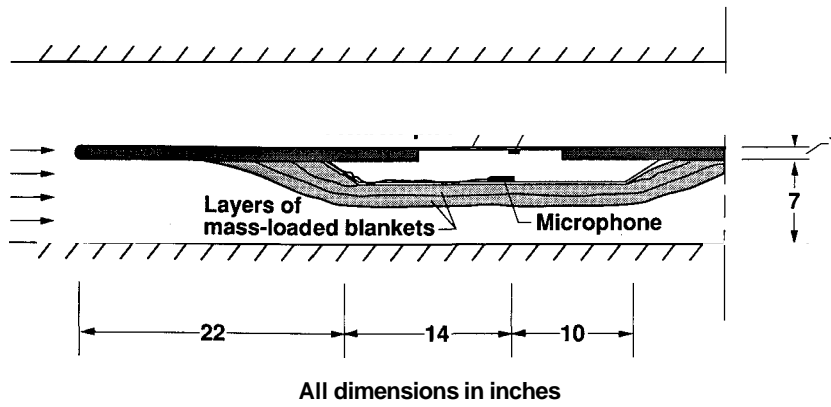


Fig. 9 Wind-tunnel test configuration of a 12 x 8 x 0.040-in. aluminum plate subjected to boundary-layer excitation.

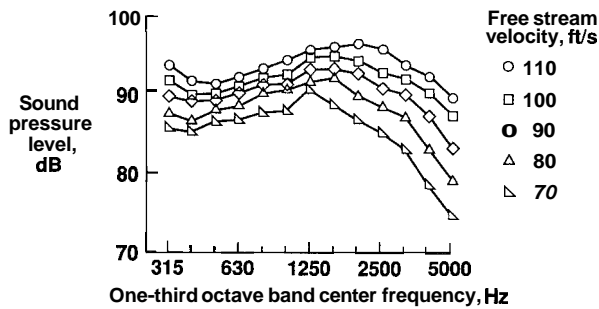


Fig. 10 Turbulent boundary-layer excitation spectra incident on the flexible aluminum plate in the wind tunnel as measured by a flush-mounted microphone at several free flow velocities.

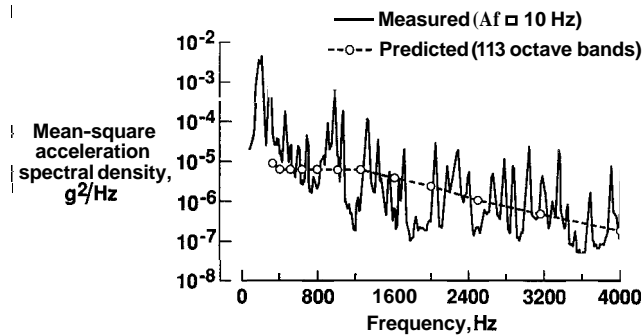


Fig. 11 Measured and VAPEPS predicted mean-square acceleration spectral density of the plate vibration in the wind tunnel due to turbulent boundary-layer excitation ($U = 90$ ft/s).

where θ is the eddy decay time. The power per unit area that is transferred from the turbulent boundary layer to the plate is derived in Ref. 21 as

$$\Pi(\omega) = \bar{P}_n^2 \frac{A_t}{R_0} \phi_f(\omega)$$

where \bar{P}_n^2 is the overall mean-square pressure, A_t is the correlation area as a function of the plate wave number, and R_0 is the admittance of an infinite plate. A typical value for the eddy decay time $\theta \approx 30\delta^*/U_c$, where δ^* is the boundary-layer displacement thickness, which is approximated as 0.125 times the boundary-layer thickness δ . The turbulent boundary-layer thickness is calculated from

$$\delta = \frac{0.37x}{Re_x}$$

where $Re_x = Ux/\nu$ is the Reynolds number at the measurement

location, x is the distance from the leading edge of the rigid plate, and ν is the kinematic viscosity.

Excitation Response

The mean-square acceleration power spectral density was calculated using the VAPEPS model for a freestream velocity of 90 ft/s and is compared with accelerometer measurements on the plate in Fig. 11. The spectrum in Fig. 10 corresponding to the 90-ft/s flow speed was used as input to the VAPEPS model. The boundary-layer thickness was calculated to be equal to 0.752 in. Reasonable agreement is obtained between the predicted and the measured acceleration levels in the frequency range 315–4000 Hz.

Analyzing other normalized mean-square acceleration plots at different speeds show that the frequencies of the individual panel modes shift to higher values as a result of an increase in flow speed. This is shown in Fig. 12 where selected modal

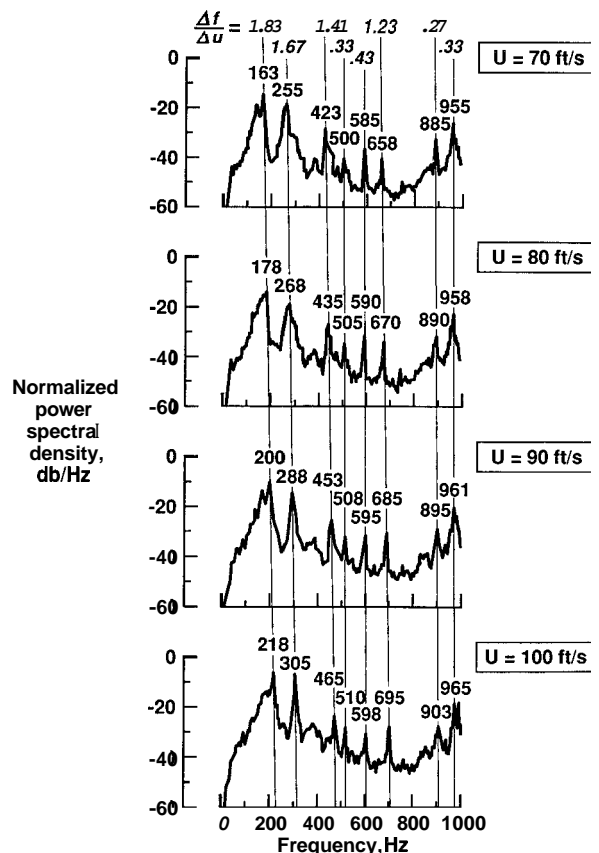


Fig. 12 Normalized acceleration spectral density of the flexible plate response at several free flow velocities.

resonance frequencies of the panel are indicated for four undisturbed flow speeds ranging from 70 to 100 ft/s. The ratio of frequency increase with freestream flow velocity is also indicated in Fig. 12 for some of the major modal responses. The ratio is highest for the fundamental plate resonance mode followed by the next couple of modes. For higher plate resonances this ratio is lower. The increase of modal frequency with flow speed was later observed for the test condition where the layers of mass-loaded blankets were removed and the air in the cavity was in open communication with the air in the flow.^{22,23}

The overall mean-square acceleration level as a function of undisturbed flow speed is plotted in Fig. 13. As mentioned earlier, boundary-layer transition over the measurement location takes place at 54.5 ft/s. The measured overall mean-square plate acceleration level in Fig. 13 seems to be linearly dependent on the undisturbed flow speed in the laminar as well as the turbulent boundary-layer flow regions. The ratio of acceleration level increase with free flow velocity for the turbulent boundary layer is approximately 0.24 dB/(ft/s). This compares well with the results of other investigators. Ffowcs-Williams and Lyon²¹ found a $U^{5.0}$ dependence of the total integrated power radiated by a panel in Ludwig's²⁴ experiments. Maestrello²⁵ also found that the acoustic power level was proportional with $U^{5.0}$ for velocities lower than Mach = 0.4. Maestrello²⁶ measured a slightly less than U^3 dependence of the root-mean-square displacement of the fundamental modes of aluminum panels subjected to turbulent boundary-layer excitation. Blake's analysis shows that a $U^{5.4}$ dependence of the mean-square displacement of the fundamental mode appears to give a good fit with the data obtained by Tack and Lambert.* It should be noted that the mean-square acceleration response is assumed to be related to the mean-square velocity by ω^2 and to the mean-square displacement by ω^4 . The overall levels in Fig. 13 are dominated by the response of the fundamental plate resonance as is evidenced by the spectra in Fig. 12. For comparison, the $U^{5.0}$ dependence curve is also plotted in Fig. 13.

The increase of the overall mean-square acceleration level with undisturbed flow speed when excited by a laminar boundary layer is shown in Fig. 13 to be equal to 0.40 dB/(ft/s), which compares with an approximated $U^{3.6}$ dependence. The ratio of the increase in overall sound pressure level, measured by the microphone in the cavity underneath the plate, to the undisturbed flow speed was found to be the same as for the plate acceleration response. This suggests that the overall transmitted sound is mainly due to the fundamental mode of vibration of the plate.

Noise Reduction

The VAPEPS model is not suited to predict sound transmission into the small space underneath the plate since the depth of this cavity is much smaller than the dimensions of the plate and the acoustic wavelength below 1000 Hz. The

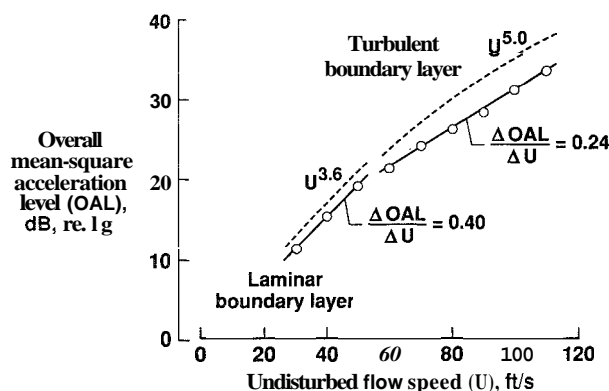


Fig. 13 Overall mean-square acceleration level of the flexible plate response as function of undisturbed flow speed.

effect of the cavity on the plate loading becomes important when it is assumed that the vibration of the plate compresses the gas inside the cavity adiabatically, thereby stiffening the plate.²⁸ However, only the odd plate modes will contribute to this effect as the volume velocities of the even plate modes cancel over the plate surface. Dowell²⁹ and also Strawderman³⁰ have analyzed this problem and found that the pressure is constant throughout the cavity. The perturbation pressure in the cavity is given by²⁹

$$p_c = \frac{\rho c_0^2}{d} \sum_{i=\text{odd}} \sum_{r=\text{odd}} A_{i,r}$$

where d is the depth of the cavity and $A_{i,r}$ is the modal amplitude of the plate vibration for mode numbers i and r . This is similar to the case of a piston driving a small air volume V in which the rms sound pressure is given by

$$\bar{p} = \frac{1}{j\omega} \left(\frac{\gamma p_s}{V} \right) \bar{Q}_0$$

where $\gamma p_s/V$ is the acoustic compliance of the gas in the enclosure and \bar{Q}_0 is the rms volume velocity of the piston. The term $1/j$ indicates that the sound pressure is 90 deg out of phase with the velocity. The noise reduction due to the plate is determined by calculating the rms pressure in the cavity from the one-third octave band mean-square acceleration response of the plate (Fig. 11) and subtracting the excitation spectrum shown in Fig. 10. Again, it was assumed that the plate acceleration was related to the plate amplitude by ω^2 . The calculations were performed for an undisturbed flow speed of 90 ft/s and a frequency region with a lower bound of 315 Hz (sufficient plate modal density) and an upper bound of 1000 Hz (cavity depth much smaller than the other cavity dimensions and the acoustic wavelength). These predictions are compared in Fig. 14 with experimentally obtained noise reduction values for the plate, which were derived from the measured sound pressure levels of the flush-mounted microphone and the microphone in the cavity. Predictions using this simple small cavity model yield reasonable agreement with the measured noise reduction. However, for cavities with dimensions larger than the acoustic wavelength, the modal behavior becomes important and the problem becomes more complicated. For sound radiation into larger spaces with higher modal density, statistical energy analysis can again be used.

Conclusions

The VAPEPS statistical energy analysis model was used in the frequency range 315–5000 Hz to predict the acceleration response and sound transmission of plates that were exposed to random acoustic or turbulent boundary-layer excitation. The noise reduction of aluminum, acrylic, and graphite-epoxy plates with dimensions of the same order or larger than the acoustic wavelength was measured in a transmission loss suite. Good agreement (within 2 dB) was obtained between the measured and VAPEPS predicted noise reduction. The modal densities of these plates as well as the acoustic modal densities of source

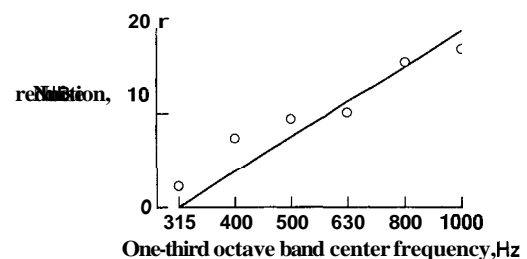


Fig. 14 Measured and predicted noise reduction of the flexible plate in the wind tunnel at a free flow velocity of 90 ft/s.

and receiver rooms were high for the frequency range considered.

The sound transmitted through a smaller ($8 \times 12 \times 0.040$ in.) aluminum plate, mounted in a 1-in. thick rigid plate in a wind tunnel, was measured for random acoustic excitation on one side of the plate and an anechoic termination on the other side. The measured data fell in between the VAPEPS predictions for resonant and nonresonant sound transmission. These results were expected because for a smaller plate the restraints at its boundaries become increasingly more important and the relative importance of resonant and nonresonant sound transmission varies with frequency.

The acceleration response of the panel was measured for the case of random acoustic excitation as well as for excitation by laminar and turbulent boundary layers at several tunnel speeds. The mean-square acceleration spectral density predicted by VAPEPS compared well with the measured plate acceleration response for excitation by a stationary (random acoustic) as well as convected (turbulent boundary layer) pressure field. Due to higher convection speeds and different eddy sizes, the resonance frequencies of the plate are shifted to higher frequencies when the undisturbed flow velocity is increased. Greater shifts were found for the lower frequency modes. The overall mean-square acceleration level increases with free flow velocity but at a different rate for the laminar than for the turbulent boundary layers. The overall acceleration level due to turbulent boundary-layer excitation was found to be close to a $U^{5.0}$ dependence as confirmed by other investigators. A similar dependence on free flow velocity was found for the overall transmitted sound pressure level. However, when the plate was excited by a laminar boundary layer, approximately a $U^{3.6}$ free flow velocity dependence was found for both the acceleration response and the transmitted sound. Finally, statistical energy analysis is not suited to predict the sound transmitted into a cavity with a depth that is small compared with the other dimensions and the acoustic wavelength. However, by virtue of the small cavity depth, a simplified theory was used that predicted the pressure inside the cavity with reasonable agreement for a frequency range from 315–1000 Hz.

References

- ¹Lyon, R. H., and Maidanik, G., "Power Flow Between Linearly Coupled Oscillators," *Journal of the Acoustical Society of America*, Vol. 34, No. 5, 1962, pp. 623–639.
- ²Maidanik, G., "Response of Ribbed Panels to Reverberant Acoustic Fields," *Journal of the Acoustical Society of America*, Vol. 34, No. 6, 1962, pp. 809–825.
- ³Lyon, R. H., "Sound Radiation from a Beam Attached to a Plate," *Journal of the Acoustical Society of America*, Vol. 34, No. 9, 1962, pp. 1265–1268.
- ⁴Lyon, R. H., and Eichler, E., "Random Vibration of Connected Structures," *Journal of the Acoustical Society of America*, Vol. 36, No. 7, 1964, pp. 1344–1354.
- ⁵Lyon, R. H., and Scharton, T. D., "Vibrational Energy Transmission in a Three Element Structure," *Journal of the Acoustical Society of America*, Vol. 38, No. 2, 1965, pp. 253–261.
- ⁶Ungar, E. E., and Scharton, T. D., "Analysis of Vibration Distributions in Complex Structures," *Shock and Vibration Bulletin*, Vol. 36, Pt. 5, 1967, pp. 41–53.
- ⁷Crocker, M. J., and Price, A. J., "Sound Transmission Using Statistical Energy Analysis," *Journal of Sound and Vibration*, Vol. 9, No. 3, 1969, pp. 469–486.
- ⁸Price, A. J., and Crocker, M. J., "Sound Transmission Through Double Panels Using Statistical Energy Analysis," *Journal of the Acoustical Society of America*, Vol. 47, No. 3, Pt. 1, 1970, pp. 683–693.
- ⁹Lee, Y. A., Henricks, W., and Park, D. M., "VibroAcoustics Payload Environment Prediction System (VAPEPS), Vol. 1: VAPEPS Improvement and Verification," NASA CR 177905, Sept. 1985.
- ¹⁰Park, D. M., "VAPEPS User's Reference Manual Version 5.0," NASA CR 180781, July 1988.
- ¹¹Park, D. M., "VAPEPS User's Guide," NASA CR 180782, July 1988.
- ¹²Badilla, G., Blitman, G., Fernandez, J., Kern, D., Rice, S., Scharton, T. D., Lee, Y. A., and Park, D. M., "VibroAcoustic Payload Environment Prediction System (VAPEPS)," Workshop Notes, Jet Propulsion Lab., California Inst. of Technology, Pasadena, CA, Feb. 15–17, 1989.
- ¹³Lee, Y. A., Crowe, D., and Henricks, W., "VAPEPS Improvement with Stress Estimation and Progressive Wave Excitation," NASA CR 180783, June 1987.
- ¹⁴Grosveld, F. W., "Characteristics of the Transmission Loss Apparatus at NASA Langley Research Center," NASA CR 172153, June 1983.
- ¹⁵Grosveld, F. W., "Field-Incidence Noise Transmission Loss of General Aviation Aircraft Double-Wall Configurations," *Journal of Aircraft*, Vol. 22, No. 2, 1985, pp. 117–123.
- ¹⁶Roussos, L. A., Powell, C. A., Grosveld, F. W., and Koval, L. R., "Noise Transmission Characteristics of Advanced Composite Structural Materials," *Journal of Aircraft*, Vol. 21, No. 7, 1984, pp. 528–535.
- ¹⁷Grosveld, F. W., and Metcalf, V. L., "Modal Response and Noise Transmission of Composite Panels," *Proceedings of the AIAA/ASME/ASCE/AHS 26th Structures, Structural Dynamics, and Materials Conference*, AIAA CR 852, Pt. 2, AIAA, New York, April 1985, pp. 617–628; also AIAA Paper 85-0789.
- ¹⁸Metcalf, V. L., and Grosveld, F. W., "Noise Transmission Characteristics of Aircraft Type Composite Panels," *Transactions of the Society of Automotive Engineers, Aircraft Structures*, No. 850878, Vol. 94, Sept. 1986, pp. 812–820.
- ¹⁹Scharton, T. D., "VAPEPS at Low Frequencies," *VAPEPS Newsletter*, No. 3, Jet Propulsion Lab., California Inst. of Technology, Pasadena, CA, Spring 1989, pp. 1–7.
- ²⁰Blake, W. K., *Mechanics of Flow Induced Sound and Vibration*, Academic Press, New York, 1986, Chap. 8, 9; pp. 497–658.
- ²¹Ffowes-Williams, J. E., and Lyon, R. H., "The Sound Radiated from Turbulent Flows Near Flexible Boundaries," Bolt, Beranek and Newman, Inc., Rept. No. 1054, Aug. 15, 1963.
- ²²Maestrello, L., and Grosveld, F. W., "Control of Boundary Layer Transition Location and Plate Vibration in the Presence of an External Acoustic Field," *Proceedings of the 4th International Conference on Structural Dynamics*, edited by M. Peyt, H. F. Wolfe, and C. Mei, Elsevier, Essex, England, UK, July 1991, pp. 702–711.
- ²³Maestrello, L., and Grosveld, F. W., "Transition Control of Instability Waves Over a Flexible Surface in the Presence of an Acoustic Field," AIAA 13th Aeroacoustics Conf., AIAA Paper 90-4008, Tallahassee, FL, Oct. 22–24, 1990; also AIAA *Journal* (to be published).
- ²⁴Ludwig, G. R., "An Experimental Investigation of the Sound Generated by Thin Steel Panels Excited by Turbulent Flow (Boundary Layer Noise)," Univ. of Toronto, UTIA Rept. 87, Toronto, Ottawa, Canada, Nov. 1962.
- ²⁵Maestrello, L., "Design Criterion of Panel Structure Excited by Turbulent Boundary Layer," *Journal of Aircraft*, Vol. 5, No. 5, 1968, pp. 321–328.
- ²⁶Maestrello, L., "Measurement and Analyses of the Response Field of Turbulent Boundary Layer Excited Panels," *Journal of Sound and Vibration*, Vol. 2, No. 3, 1965, pp. 270–292.
- ²⁷Tack, D. H., and Lambert, R. F., "Response of Bars and Plates to Boundary-Layer Turbulence," *Journal of Aeronautical Sciences*, Vol. 29, 1962, pp. 311–322.
- ²⁸Dowell, E. H., and Voss, H. M., "The Effect of a Cavity on Panel Vibration," *AIAA Journal*, Vol. 1, No. 2, 1963, pp. 476–477.
- ²⁹Dowell, E. H., "Transmission of Noise from a Turbulent Boundary Layer Through a Flexible Plate into a Closed Cavity," *Journal of the Acoustical Society of America*, Vol. 46, No. 1 (Pt. 2), 1969, pp. 238–252.
- ³⁰Strawderman, W. A., "The Acoustic Field in a Closed Space Behind a Rectangular Simply Supported Plate Excited by Boundary Layer Turbulence," U.S. Navy Underwater Systems Center, Rept. 827, Fort Trumbell, New London, CT, May 1967.